vehicles

MDPI

Article

Intelligent Fault Diagnosis in Gasoline Engines Using Convolutional Neural Networks

Rogelio Santiago León-Japa [1,*], Lainny Josue Yagloa-Tarco [2], Anthony Joel Vinueza-Soria [2], Juan Pablo Medina-Namicela [3] and José Luis Maldonado-Ortega [4]

[1] Department of Electrical Engineering, University of Jaén, EPS Linares, 23700 Jaén, Spain
[2] Automotive Engineering Career, Politecnica Salesiana University, Guayaquil 090109, Ecuador; lyagloa@est.ups.edu.ec (L.J.Y.-T.); avinuezas2@est.ups.edu.ec (A.J.V.-S.)
[3] Department of Automotive Engineering, Faculty of Energy, Industries and Non-Renewable Natural Resources, National University of Loja, Guillermo Falconí University Campus, Loja 110103, Ecuador; juan.p.medina.n@unl.edu.ec
[4] GMOVINT Research Groups, Automotive Engineering Career, Politecnica Salesiana University, Guayaquil 090109, Ecuador; jmaldonadoo@ups.edu.ec
* Correspondence: rslj0001@red.ujaen.es

Abstract

This research focuses on the application of convolutional neural networks (CNNs) for fault detection in ignition coils and fuel injectors of a YESA 3140 gasoline engine. The objective is to design a CNN capable of identifying when the spark ignition engine (SIE) is operating under optimal conditions and when it presents specific power supply disconnection faults in the four injectors and four coils. Signals from the knock sensor (KS) and camshaft position sensor (CMP) of the SIE were acquired using a MyDAQ data acquisition card and LabVIEW software version 2024. A strict sampling protocol was followed: each replicate had a duration of 5 s while the engine was running at normal operating temperature and idle speed. Prior to each sampling, the SIE was operated with the corresponding fault induced for 5 min. The signals obtained from the KS sensor were transformed into spectrograms, which were then used to train various CNN models. The resulting CNN achieved a classification error of 3.21%. The algorithm was validated by inducing supervised faults in various Otto cycle engines.

Keywords: CNN; MEP; electrical faults; ignition coils; fuel injectors; diagnosis

Academic Editors: Longda Wang, Guibing Zhu and Chuanfang Xu

Received: 5 March 2026
Revised: 13 April 2026
Accepted: 28 April 2026
Published: 2 June 2026

1. Introduction

Early detection of faults in vehicle drive systems is important for ensuring good performance and extending the service life of spark ignition engines (SIE). According to data from the National Institute of Statistics and Census (INEC), there are 29,068 entities related to the automotive sector in Ecuador, and approximately 70% of them are dedicated to maintenance and repair services [1]. Despite this, in cities such as Guayaquil, many workshops still use conventional diagnostic methods that rely mainly on the technician's experience. This dependence on subjective criteria can lead to errors in identifying faults and even to unnecessary mechanical interventions [2].

Over time and with continuous use, spark ignition engines (SIE) are susceptible to a wide range of mechanical failures caused by component wear, material degradation, or severe operating conditions. These factors compromise not only engine efficiency but also cause an increase in pollutant emissions. In this context, the timely detection of anomalies

in PIE engines is important for maintaining their functionality, improving their operational safety, and reducing their environmental impact [2,3]. In general, the diagnosis of faults in MEP engines not only seeks to increase the reliability and efficiency of the system, but also to promote the development of advanced technologies that respond to the growing complexity of modern automotive systems [4,5].

Within this context, machine learning is proposed as a methodology for fault diagnosis, since it is an artificial intelligence technique that deals with the design and development of algorithms capable of solving specific tasks using patterns from a database and applying them to make decisions [6–8]. In the field of machine learning, artificial neural networks (ANNs) have shown outstanding performance in identifying both mechanical and electrical faults in spark ignition engines (SIE) [9–11]. Thanks to their learning and generalization capabilities, these techniques have positioned themselves as an effective alternative for the implementation of intelligent systems aimed at real-time diagnosis and early fault detection [12]. Similarly, their contribution has been key to improving operational reliability and strengthening predictive maintenance strategies in this type of machine [13,14].

Within the field of machine learning, deep learning has gained relevance due to its ability to interpret and learn complex patterns in large volumes of data [15,16]. On the other hand, one of the most representative architectures of this approach is convolutional neural networks (CNN), which are derived from the traditional artificial neural network model but are distinguished by operating mainly with images as a data source, making them particularly effective in visual recognition tasks [17].

The basic architecture of a convolutional neural network consists of multiple layers that perform specific operations within the learning process. Among these is the Rectified Linear Unit (ReLU) activation function, which introduces non-linearity into the model and allows both positive and negative values to be processed, thus promoting more efficient convergence during network training. Finally, the network has an output layer that delivers the system's response based on the processed patterns [6]. Convolutional neural networks (CNNs) have established themselves as an effective alternative in fault detection, thanks to their ability to process complex visual data, automatically identify patterns, and facilitate the early detection of anomalies in dynamic systems [17–20].

In recent years, deep learning techniques have significantly improved fault diagnosis performance due to their ability to automatically extract complex patterns from raw data. In particular, convolutional neural networks (CNNs) have shown strong capabilities in processing time–frequency representations such as spectrograms, enabling the identification of fault-related features without manual feature engineering. Several studies have demonstrated the effectiveness of CNN-based approaches in vibration and acoustic signal analysis for fault diagnosis in mechanical systems [11–22].

The use of spectrograms as input to CNN models has become a widely adopted strategy in fault diagnosis, as it allows transforming one-dimensional signals into two-dimensional representations that capture both temporal and frequency-domain information. This approach enhances feature separability and improves classification performance compared to traditional signal-based methods. Previous research has validated the effectiveness of this representation in diagnosing faults in rotating machinery and automotive systems [15–23].

This study adopts an important approach using machine learning for the identification and classification of faults related to the ignition coils and injectors of an MEP [12]. Fault diagnosis using machine learning techniques is usually based on data obtained from various sensors installed in the drive system [24]. In particular, this research uses information from the knock sensor (KS) and the camshaft position sensor (CMP), which allow relevant signals from the engine's operating behavior to be captured. Based on this data, an

artificial neural network (ANN) with its own architecture was designed, following the feed-forward backpropagation approach, widely recognized for its ability to model complex dynamics [25–27]. This type of ANN represents an effective alternative to traditional diagnostic methods, offering greater accuracy and adaptability [28].

In addition to machine learning-based approaches, fault diagnosis in spark ignition engines has also been addressed through physics-based models, advanced signal processing techniques such as wavelet transform, frequency domain analysis, and expert systems. These approaches allow for the identification of anomalies based on mathematical models of the system or by extracting specific features from the signals. However, they have limitations in environments with high operational variability or when precise system models are not available.

In this context, the present study proposes a fault diagnosis approach based on convolutional neural networks (CNN), using spectrograms derived from knock sensor (KS) signals. The proposed methodology enables the classification of nine operating conditions, including normal operation and eight fault scenarios related to ignition coils and fuel injectors. The main contribution of this work lies in the integration of time–frequency signal analysis with deep learning techniques under a structured experimental framework, providing a reproducible approach for intelligent fault diagnosis in spark ignition engines.

This article is organized as follows: Section 2 describes the materials, data acquisition, and methodology used; Section 3 presents the results obtained; Section 4 discusses the findings in comparison with previous work; finally, Section 5 presents the conclusions and future research directions.

2. Materials and Methods

2.1. Experimental Unit

The engine used in this research is a YESA 3140 model, whose technical specifications are detailed in Table 1. Prior to sampling, the correct operation of the test bench was verified and it was ensured that the operating conditions of the engine were stable and representative of actual behavior. This was done in order to obtain reliable, high-quality data and avoid capturing signals resulting from an abnormal state different from that of the sampling.

Table 1. Especificaciones técnicas del motor YESA 3140.

Characteristics	Specifications
Model	NF Sonata (Hyundai Motor Company (Seoul, Republic of Korea))
Valve train system	DOHC
Displacement	2.0 L
Compression ratio	10.5
Fuel system	Indirect gasoline injection
Power	143 HP @ 6000 RPM
Torque	188 Nm @ 4250 RPM

Engine used for research.

2.2. Sensors Used for Data Acquisition

The signals corresponding to the KS and CMP sensors were recorded, which allow, respectively, to detect the vibration generated by the engine under different operating conditions and to identify the phases of the working cycle of a spark ignition engine (SIE) [13]. Once the sensors were defined, their signals were validated using an oscilloscope. The waveforms of the KS and CMP sensor signals have a sampling interval of 5000 ms

and a scale of 50 mV per division. This verification confirmed the accuracy of the signals acquired before processing.

Once the instrumentation system was connected, the operating conditions to which the experimental unit would be subjected were defined. To do this, an experimental plan was designed in Minitab software version 21, which included two replicates per treatment and initially generated a total of 32 combinations. However, scenarios corresponding to combined failures of both injectors and ignition coils were excluded due to their low representativeness and practical relevance [29]. As a result, nine experimental treatments were established, each with 10 repetitions to ensure the statistical validity of the data [12,13]. The defined treatments are detailed in Table 2.

Table 2. Functional conditions for the experimental unit.

N°	Condition	Identifier
1	Engine operating normally	100
2	Coil failure 1	200
3	Coil failure 2	300
4	Coil failure 3	400
5	Coil failure 4	500
6	Injector failure 1	600
7	Injector failure 2	700
8	Injector failure 3	800
9	Injector failure 4	900

Each condition is identified.

2.3. Implementation

Data acquisition involved the use of sensors, DAQ cards, and a computer equipped with LabVIEW software, which is a graphical programming interface on a PC for more robust, versatile, and affordable measurement [5]. In general, the instrumentation used consists of: the YESA 3140 experimental unit, a G-Scan 2 automotive scanner, KS and CMP sensors, a MyDAQ data acquisition card, and a laptop computer. Figure 1 shows both the instrumentation described and the flow of data from the experimental unit to the computer.

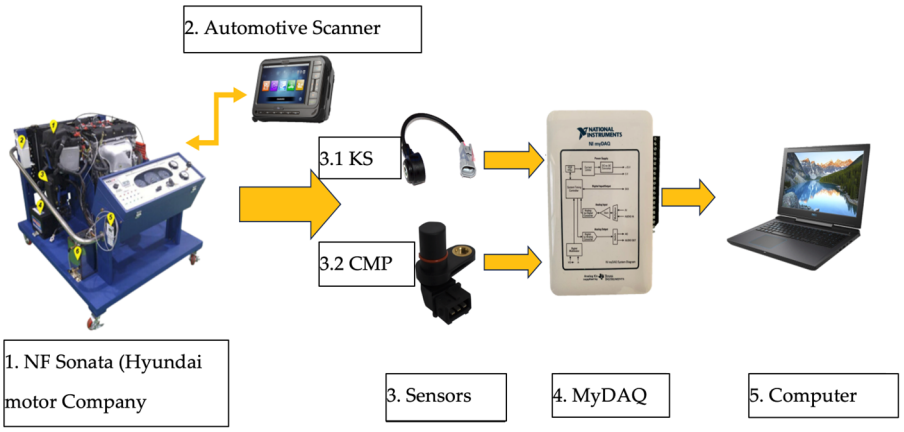

Figure 1. Instrumentation for data collection.

2.4. Instrumentation for Data Acquisition

LabVIEW software, configured according to technical references from specialized literature, was used for data acquisition and storage in Excel (.xls) format. The acquisition system was set with a sampling frequency of 20 kHz and blocks of 1000 samples per read. Under a continuous acquisition mode, this configuration allows approximately 20,000 data

points to be recorded per second, since multiple sequential reads are performed within each second. This approach ensures adequate temporal resolution for capturing the knock phenomena occurring within the engine cylinders, while maintaining efficient data handling during acquisition. The sampling frequency of 20 kHz complies with Nyquist's criterion, which establishes a minimum data acquisition rate of twice the maximum frequency of the phenomenon to be captured. In the specific case of the KS sensor, whose characteristic frequency is 9.35 kHz, the minimum value required according to this criterion would be 18.7 kHz. Therefore, the selected frequency guarantees accurate signal reconstruction. Additionally, an input range for the analog signal was set between −5 V and +5 V to capture the complete duty cycle of the signals emitted by the sensors.

Data acquisition followed a systematic protocol. First, the operating condition corresponding to the MEP was applied and left to run continuously for a period of five minutes. Subsequently, using an automotive scanner, it was verified that the spark ignition engine (MEP) was operating at idle speed and had reached a stable operating temperature between 90 °C and 95 °C [28]. Once these criteria were met, the signal was recorded for a five-second interval for each of the experimental conditions defined in Table 2. Ten replicates were sampled for each condition [12]. The complete data acquisition procedure is described in the flowchart in Figure 2. The meteorological conditions and weather conditions under which the samples were taken were: ambient temperature of 28 °C to 31 °C and atmospheric pressure of 1007 hPa.

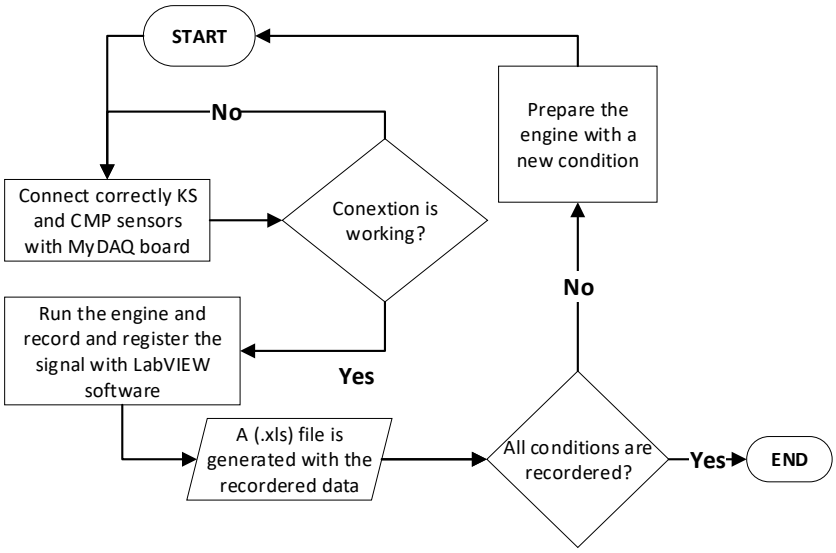

Figure 2. Process flowchart for data acquisition.

2.5. Data Processing

For data processing, a script was developed in Matlab that allowed a total of 280 samples to be extracted for each engine operating condition. Each sample was stored in ".mat" format and contained 3553 data points from the knock sensor (KS). Figure 3a shows the flowchart summarizing the procedure prior to the introduction of the data into the convolutional neural network (CNN). The process began with the dataset recorded in .xls format, in which the recorded signals from the KS and CMP sensors were organized into columns. Subsequently, using processing tools in Matlab, the data was reorganized and converted to ".mat" format to optimize its use in deep learning environments.

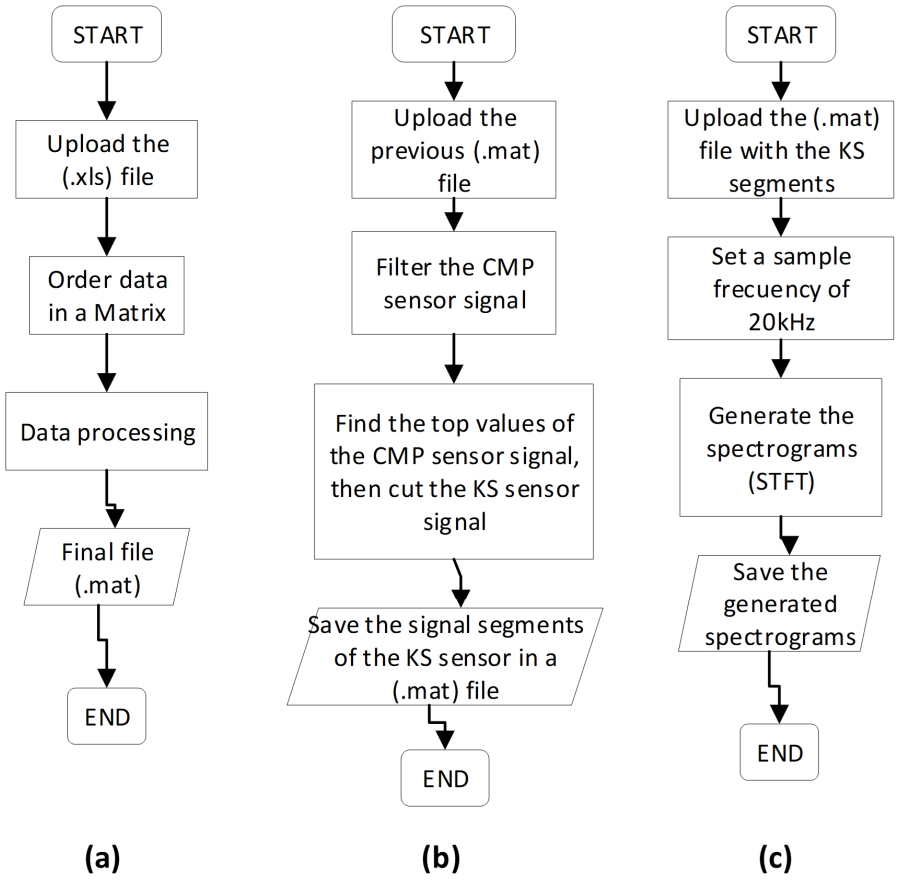

Figure 3. Flowchart (**a**) data conversion process, (**b**) signal segmentation process, (**c**) obtaining the spectrogram.

2.6. KS Sensor Signal Segmentation

Figure 3b shows the flowchart describing the procedure carried out for signal analysis and segmentation. The process began with the loading of data corresponding to the CMP and KS sensors. Subsequently, a Butterworth filter was applied to the CMP signal in order to reduce noise and improve the detection of relevant events. After filtering the signal, the significant peaks of the CMP were identified, which defined the period associated with a complete engine cycle. In each recorded sample, 26 peaks were detected, therefore, 25 cuts were made for each one. With 10 samples for each condition, 250 signal segments were obtained for each treatment. Finally, each segment was stored individually in ".mat" format files for subsequent input into the CNN algorithm.

2.7. Conversion of Signal Segments into Spectrograms

Figure 3c shows the flowchart for processing the signal from the knock sensor (KS). The process began by loading the file that stores the information collected by the sensor. Next, the signal spectrogram was calculated and its scale was converted to decibels (dB) to generate a color map that allowed the variation in power to be visualized as a function of time and frequency.

Each spectrogram generated was exported in ".png" image format, and this process was automated using a script developed in Matlab. In this way, the set of images needed to train the convolutional neural network (CNN) was systematically generated.

As a result of the process, spectrograms were obtained. Figure 4 shows one of them, which represents a two-dimensional matrix whose horizontal axis corresponds to the time and the vertical axis to the frequencies contained in the signal, with the low-frequency

components located at the bottom and the high-frequency components at the top. The color scale represents the third dimension and indicates the amount of energy contained in the signal at each point, or the spectral power density expressed in decibels (dB).

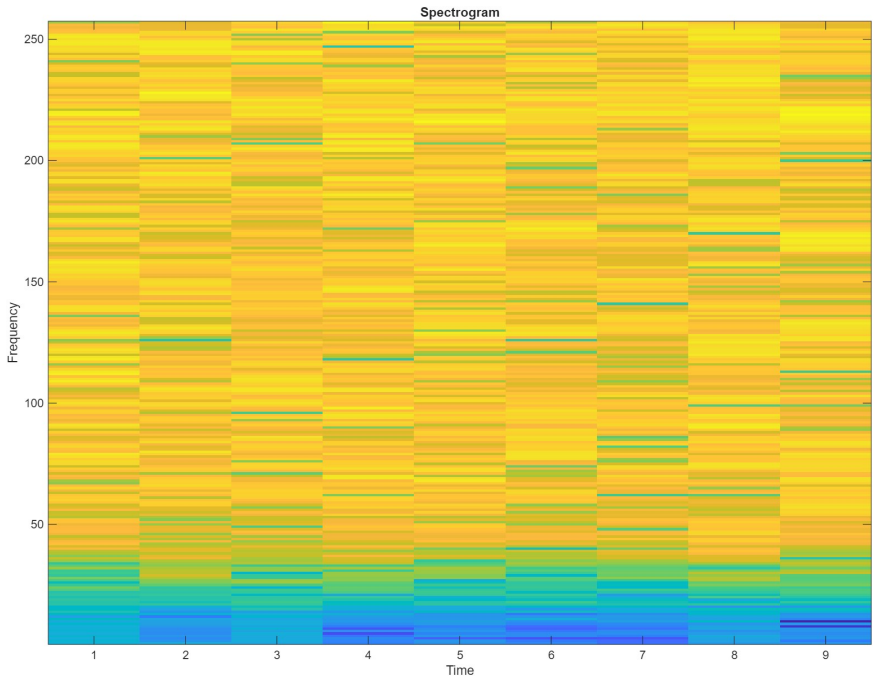

Figure 4. Spectrogram graph generated from a fragment of the KS sensor signal.

The spectrogram is constructed from segments of the signal contained within a parameter known as a "time window." The window moves along the original signal to obtain different fragments as time progresses. Thanks to this method, it was possible to clearly observe the behavior of the spectral content throughout the recorded period.

2.8. Design and Training of the Convolutional Neural Network

The convolutional neural network (CNN) was designed for classifying spectrograms obtained from signals of the detonation sensor (KS). As input, 224 × 224 pixel images with three color channels were used. The network architecture consists of multiple convolutional layers with 3 × 3 filters and same padding, organized into blocks that include batch normalization and ReLU activation functions. Initially, 16 filters were employed, gradually increasing to 56 filters in the deeper layers, which allowed for the extraction of hierarchical features from the spectrograms. To reduce dimensionality and select relevant features, MaxPooling layers with 3 × 3 and 2 × 2 windows were incorporated. Subsequently, two fully connected layers with 256 and 128 neurons were included, respectively, followed by an output layer with 9 neurons, corresponding to the evaluated operating conditions. The final classification was performed using a softmax function.

Figure 5a shows the flowchart corresponding to the procedure implemented for the design, training, and validation of the convolutional neural network (CNN). The first step involved loading the database containing the previously generated spectrograms, which were used in both the training and validation stages of the model.

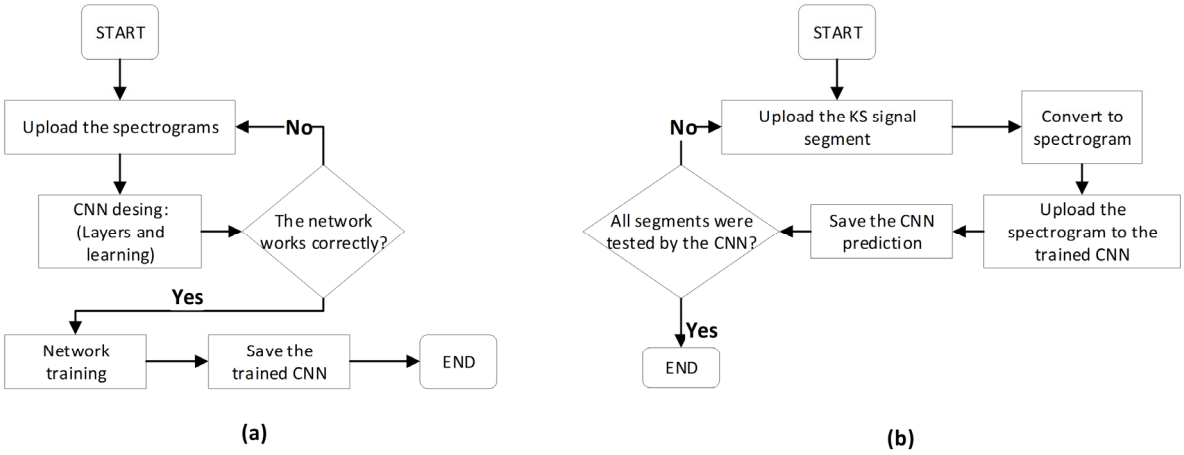

Figure 5. Flowchart (**a**) CNN training, (**b**) CNN validation.

Once the architecture of the convolutional neural network (CNN) was defined, the model was trained using the generated spectrograms. The network consists of an input layer, multiple convolutional layers with ReLU activation functions, reduction layers through MaxPooling, and a final classification layer. This structure allows for the progressive extraction of features, from simple patterns like edges and textures to more complex representations associated with the engine's operating conditions.

MaxPooling layers reduce the dimensionality of the data, preserving the most relevant information and improving computational efficiency. This iterative process across different layers facilitates the extraction of high-level features that are used in the classification stage.

During training, the model's performance was evaluated using accuracy (mini-batch accuracy) and the loss function (mini-batch loss), as shown in Table 3. A progressive improvement in accuracy was observed as the iterations advanced, starting from 25% and reaching values close to 100% in the final stages of training. After a re-training process, an approximate variation of 4% in accuracy was observed, indicating consistency in the model's behavior. Additionally, the loss values corresponding to the iterations with the highest accuracy were analyzed, resulting in an average value of 3.21%, which represents the proportion of information not captured by the network during the learning process.

Table 3. CNN training results.

Iteration	Mini-Batch Accuracy (%)	Mini-Batch Loss	Learning Rate
1	25.00	19.1740	0.0010
12	18.75	21.8861	0.0010
34	90.62	0.5216	0.0010
36	100.00	0.2192	0.0010
39	96.88	0.0770	0.0010
40	96.88	0.1638	0.0010
42	100.00	0.0649	0.0010
44	100.00	0.0292	0.0010
46	100.00	0.0022	0.0010

The chart shows the iterations with the most significant changes.

Finally, once the convolutional neural network (CNN) was trained, it was implemented as a diagnostic system aimed at detecting faults in the ignition coils and engine injectors. Its operation was validated by identifying the different operating conditions of the engine, and its ability to identify patterns associated with normal and abnormal operating states was verified.

Figure 5b shows the flowchart for the fault diagnosis system validation process. At this stage, the test samples are loaded in spectrogram format and entered into the previously trained convolutional neural network. Once processed by the network, it outputs the classification of the engine's operating condition, allowing the accuracy and effectiveness of the developed system to be verified.

3. Results

The results obtained from the model validation are presented in Figure 6, where the confusion matrix shows that the neural network correctly classified all the validation samples for the detection of each fault, indicating that the CNN was able to identify the different engine states.

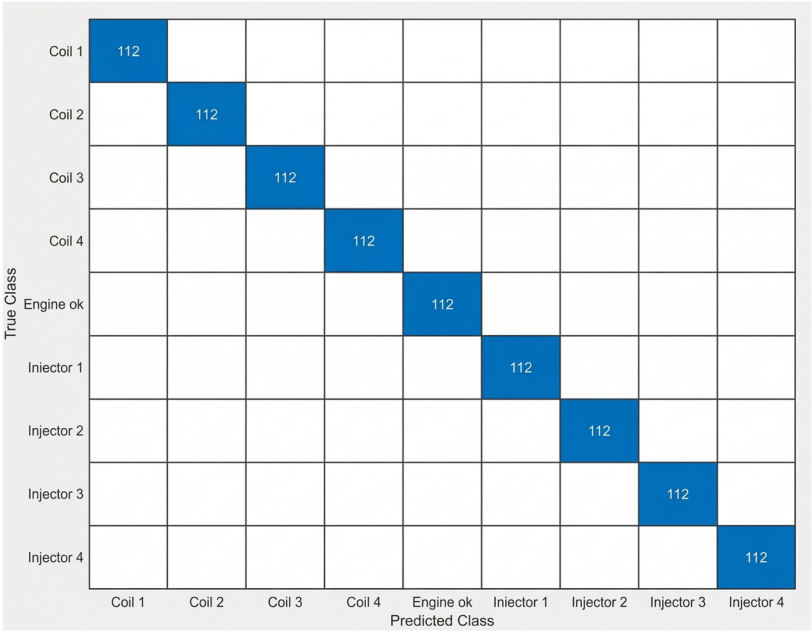

Figure 6. Confusion matrix.

Additionally, the matrix shown in Figure 6 displays the results of fault classification using the proposed model and reflects that the CNN performs optimally in identifying the different operating conditions of the motor. There is a very precise match between the actual and predicted categories, with a total of 112 correct predictions in each class, suggesting that the system is able to accurately differentiate between faults in coils, injectors, and the engine in optimal operation. The diagonal arrangement of the values in the matrix indicates an error-free classification, which validates the model's ability to distinguish with high certainty between different operating conditions. This result reinforces the reliability of the implemented approach and its applicability in real automotive diagnostic environments.

Figure 7 shows an interface developed in LabVIEW, designed to validate the processed samples against the original data. The display distinguishes two main sections: one corresponding to the initial samples and the other to the trained samples. The system incorporates a cylinder identifier that allows the fault to be located within the four cylinders of the engine, highlighting in red the one where the anomaly is detected. In addition, a section is included that shows the status assigned to each condition and the corresponding fault code, which facilitates the accurate classification of the different types of faults identified during the diagnostic process.

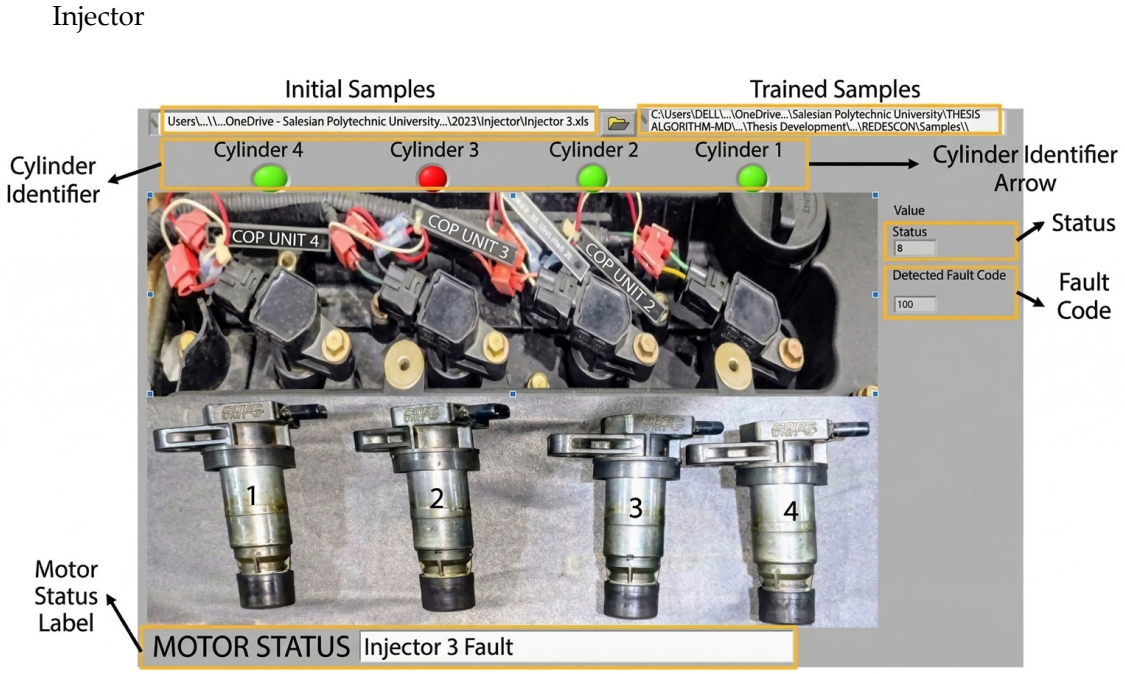

Figure 7. Verification of fuel injector failure in MEP with interface development in Labview.

An analysis of variance (ANOVA) was used in Minitab software to check the consistency between the responses obtained by the convolutional neural network (CNN) and the actual behavior of the engine during operation. It was found that both belong to the same grouping category (A), suggesting a strong match between the actual data and what the model predicts. In addition, the statistical significance value obtained (p-value = 0.953) shows that the results obtained from the CNN have a confidence level of between 95.3% and 98%.

Figure 8a shows that when the data is grouped and Tukey's method is applied, there is a 95% confidence index between the responses obtained from the CNN and the actual condition of the MEP. It is concluded that the means are equivalent and there is no significant difference. For this reason, it is confirmed that the means of each of the responses coincide at a value close to zero. Similarly, Figure 8b shows the interval graph that demonstrates that the tests under the actual operating conditions of the MEP and the prediction generated by the neural network are statistically equivalent, given that the 95% confidence intervals overlap significantly. Thus, it is verified that the model has a good fit and that its predictions do not differ significantly from the system values. Finally, Figure 8c shows the graphs obtained from residuals under real conditions, with the aim of verifying the statistical assumptions of the proposed model. Thus, the normal probability graph shows an approximately linear distribution of the residuals, indicating that they conform to a normal distribution. For its part, the histogram graph reflects a symmetrical dispersion around zero, which reinforces this normality. Similarly, the graph of residuals versus adjusted values does not show any defined patterns, indicating homogeneity of variance. Finally, the analysis of residuals as a function of the order of observation indicates a random distribution, without systematic trends, suggesting that there is no temporal correlation between them. Taken together, these results support the validity of the model and provide reliability of its estimates under real operating conditions.

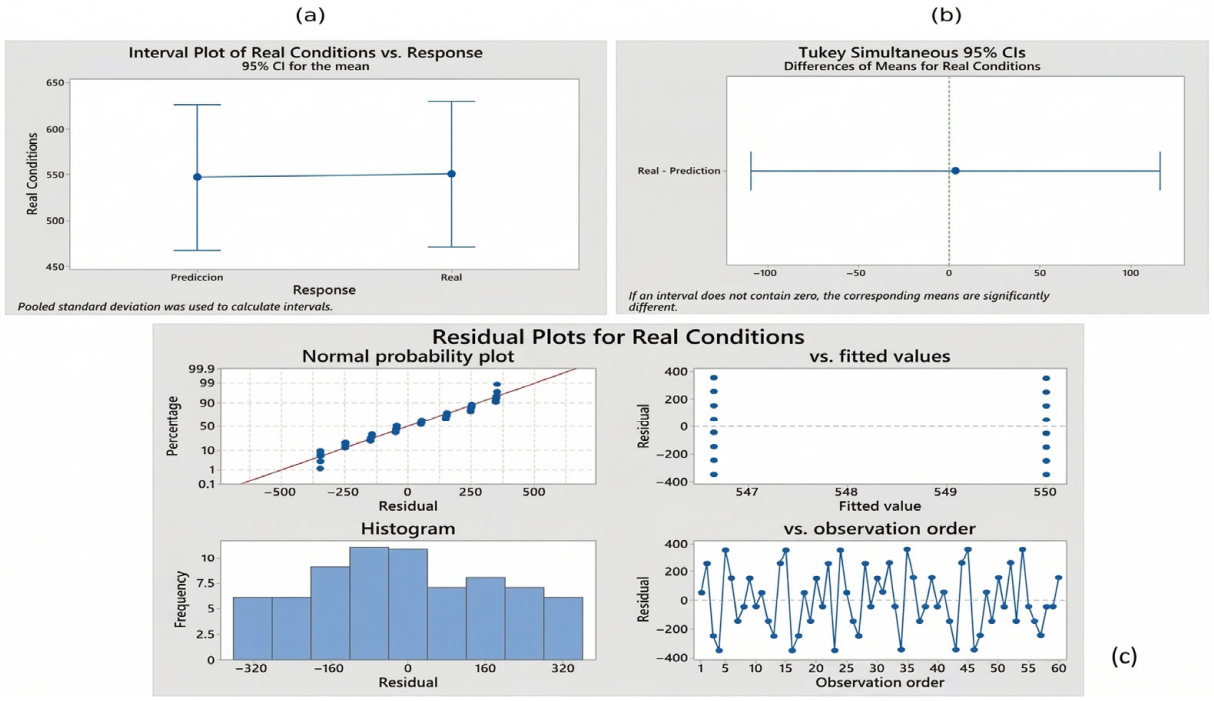

Figure 8. Graph (**a**) differences in means, (**b**) data intervals, (**c**) residual analysis.

4. Discussion

Results obtained in this research confirm that convolutional neural networks (CNN) are a highly effective tool for detecting faults in spark ignition engines (SIE) and achieve a high level of accuracy. This result shows that the model can effectively recognize and capture patterns that allow it to distinguish between specific faults in the ignition coils (cylinders 1, 2, 3, and 4) and in the corresponding fuel injectors.

The CNN demonstrated outstanding performance in terms of classification, with minimum error margins of 6%, 2%, and 0.2%, respectively. When comparing these results with previous studies such as [1,5,25], it is confirmed that, in general terms, neural networks perform better in data classification tasks, especially under different operating conditions of a spark ignition engine.

In comparison, the error percentages reported in previous research 0.0082% [5], 3.64% [30], 0.1267% [25], and 0.3335% for support vector machines (SVM) [13] with the information loss value obtained in this study (3.21%), it is evident that the CNN model developed is within acceptable margins and comparable to previously validated methodologies. Consequently, it is concluded that CNNs represent a viable and effective alternative for the automatic classification of faults in MEP engines.

In addition, recent research has demonstrated the effectiveness of integrating time–frequency signal representations with deep learning models for fault diagnosis in mechanical systems. The use of spectrograms as input data allows convolutional neural networks to simultaneously capture temporal and frequency-domain characteristics, enhancing their ability to discriminate between different fault conditions. Studies such as those by Yoo et al. [21] and Zheng et al. [22] have shown that this approach improves classification performance in vibration-based diagnostics. Likewise, Qiu et al. [11] reported that deep learning methods, particularly CNNs, surpass traditional machine learning techniques due to their capacity for automatic hierarchical feature extraction, eliminating the need for manual feature engineering.

5. Conclusions

The CNN network was structured with an input layer, followed by ReLU activation functions, dimension reduction layers using MaxPooling, and finally an output layer responsible for classification. This configuration allows 100% accuracy in fault classification, with a minimum information loss of 3.21%.

Using one-way analysis of variance (ANOVA), it is demonstrated that there is no statistically significant difference between the actual fault classification and the results obtained by the convolutional neural network (CNN). The value of $p = 0.953$ supports this statement, indicating a high correspondence between both responses, which validates the accuracy of the model in identifying motor faults.

This paper shows the acquisition of data from the KS and CMP sensors using a MyDAQ acquisition card and LabVIEW software, configured with a sampling frequency of 20 kHz. This configuration provided sufficient information to generate spectrograms, which were used in the training and validation stages of the convolutional neural network (CNN).

This work contributes to the advancement of diagnostic methods that do not require physical intervention on the engine, which avoids having to dismantle parts to detect faults, something that is still common in several workshops in Guayaquil. In this sense, the use of a non-CNN not only optimizes diagnostic times, but also offers a more economical, accurate, and efficient alternative for detecting faults in injection and ignition systems.

The results achieved demonstrate that the use of convolutional neural networks is an effective option for automatically identifying faults in the ignition coils and injectors of a spark ignition engine (SIE), using only the signal from the KS sensor. Unlike other approaches, including conventional neural networks, CNNs have the advantage of handling large amounts of data without negatively affecting their performance, as they do not usually present problems of saturation or loss of performance.

Author Contributions: Conceptualization, R.S.L.-J.; methodology, R.S.L.-J., L.J.Y.-T. and A.J.V.-S.; software, L.J.Y.-T., A.J.V.-S. and J.L.M.-O.; validation, R.S.L.-J., J.L.M.-O. and L.J.Y.-T.; formal analysis, R.S.L.-J., L.J.Y.-T. and A.J.V.-S.; research, R.S.L.-J., L.J.Y.-T. and A.J.V.-S.; resources, R.S.L.-J., L.J.Y.-T. and A.J.V.-S.; data curation, L.J.Y.-T., A.J.V.-S. and J.L.M.-O.; drafting of the original manuscript, R.S.L.-J., L.J.Y.-T., A.J.V.-S. and J.P.M.-N.; review and editing, R.S.L.-J. and J.L.M.-O.; visualization, R.S.L.-J.; supervision, R.S.L.-J., J.L.M.-O. and J.P.M.-N.; project management, R.S.L.-J. and J.L.M.-O.; fundraising, J.L.M.-O. All authors have read and agreed to the published version of the manuscript.

Funding: This research did not receive external funding. Publication costs will be covered by the authors.

Data Availability Statement: The original contributions presented in this study are included in the article. Further inquiries can be directed to the corresponding author.

Conflicts of Interest: The authors declare no conflict of interest.

References

1. Peña, A.; Pinta, F.; Angulo, N.; Sosa, B. Análisis Sectorial Guayas y Pichincha Lideran el Mercado del Sector Automotriz en Ecuador. Análisis Sectorial Automotriz y Autopartes. 2011. Available online: https://www.ecuadorencifras.gob.ec/wp-content/descargas/Infoconomia/info7.pdf (accessed on 1 April 2024).
2. Arichávala, A.; Jerez, C. Diseño e Implementación de un Software para Adquisición y Visualización de Parámetros Funcionales del Banco Dinamométrico Marca Armfield Modelo CM11. Bachelor's Thesis, Universidad Politécnica Salesiana, Guayaquil, Ecuador, 2017. Available online: https://dspace.ups.edu.ec/handle/123456789/15068 (accessed on 8 July 2025).
3. Dominka, S.; Tabrizi, S.; Mandl, M.; Dubner, M. Automotive Feature Coordination based on a Machine-Learning Approach. In Proceedings of the 2021 IEEE 11th Annual Computing and Communication Workshop and Conference, CCWC 2021, Las Vegas, NV, USA, 27–30 January 2021; pp. 726–731. [CrossRef]
4. Checa, A. Desarrollo de un Modelo Basado en Redes Neuronales Artificiales Para la Predicción de Emisiones Contaminantes en un Motor Diésel DI. July 2019. Available online: https://riunet.upv.es/handle/10251/124203 (accessed on 5 March 2026).

5. Garzón, G.; Urdiales, M. Diseño e Implementación de un Sistema Para Determinar Fallas Mecánicas en Motores de Encendido Provocado Mediante Redes Neuronales Artificiales. 2017. Available online: http://dspace.ups.edu.ec/handle/123456789/14397 (accessed on 5 March 2026).
6. Mathworks. Introducción a Machine Learning—MATLAB & Simulink. 2025. Available online: https://la.mathworks.com/discovery/machine-learning.html (accessed on 5 March 2026).
7. Li, J.; King, S.; Jennions, I. Intelligent Fault Diagnosis of an Aircraft Fuel System Using Machine Learning—A Literature Review. *Machines* **2023**, *11*, 481. [CrossRef]
8. Zhang, X.; Hua, X.; Zhu, J.; Ma, M. Intelligent Fault Diagnosis of Liquid Rocket Engine via Interpretable LSTM with Multisensory Data. *Sensors* **2023**, *23*, 5636. [CrossRef] [PubMed]
9. Tao, J.; Qin, C.; Li, W.; Liu, C. Intelligent Fault Diagnosis of Diesel Engines via Extreme Gradient Boosting and High-Accuracy Time–Frequency Information of Vibration Signals. *Sensors* **2019**, *19*, 3280. [CrossRef] [PubMed]
10. Xie, F.; Li, G.; Hu, W.; Fan, Q.; Zhou, S. Intelligent Fault Diagnosis of Variable-Condition Motors Using a Dual-Mode Fusion Attention Residual. *J. Mar. Sci. Eng.* **2023**, *11*, 1385. [CrossRef]
11. Qiu, S.; Cui, X.; Ping, Z.; Shan, N.; Li, Z.; Bao, X.; Xu, X. Deep Learning Techniques in Intelligent Fault Diagnosis and Prognosis for Industrial Systems: A Review. *Sensors* **2023**, *23*, 1305. [CrossRef] [PubMed]
12. Contreras, W.; Maldonado, J.; León, R. Aplicación de una red neuronal feed-forward backpropagation para el diagnóstico de fallas mecánicas en motores de encendido provocado. *INGENIUS* **2019**, *2019*, 32–40. [CrossRef]
13. Delgado, E. Desarrollo de un Algoritmo de Diagnóstico para la Detección de Fallas Mecánicas en Motores de Encendido Provocado Basados en la Transformada Wavelet. 2018. Available online: http://dspace.ups.edu.ec/handle/123456789/15300 (accessed on 5 March 2026).
14. Kisic, E.A.; Petrovic, V.V. Application of neural network for detection and classification of faults in gasoline internal combustion engine. In Proceedings of the 2020 28th Telecommunications Forum (TELFOR), Belgrade, Serbia, 24–25 November 2020. [CrossRef]
15. Zhao, J.; Yuan, M.; Cui, Y.; Cui, J. A Cross-Machine Intelligent Fault Diagnosis Method with Small and Imbalanced Data Based on the ResFCN Deep Transfer Learning Model. *Sensors* **2025**, *25*, 1189. [CrossRef] [PubMed]
16. Saha, D.K.; Hoque, M.E.; Badihi, H. Development of Intelligent Fault Diagnosis Technique of Rotary Machine Element Bearing: A Machine Learning Approach. *Sensors* **2022**, *22*, 1073. [CrossRef] [PubMed]
17. Santillana, S. Introducción a las Redes Neuronales para el Tratamiento de Imágenes. 2022. Available online: https://digibug.ugr.es/bitstream/handle/10481/76426/libro%281%29.pdf?sequence=1&isAllowed=y (accessed on 5 March 2026).
18. Arista-Jalife, A.; Calderón-Auza, G.; Fierro-Radilla, A.; Nakano, M. Clasificación de Imágenes Urbanas Aéreas: Comparación entre Descriptores de Bajo Nivel y Aprendizaje Profundo. *Inf. Tecnológica* **2017**, *28*, 209–224. [CrossRef]
19. Janssens, O.; Slavkovikj, V.; Vervisch, B.; Stockman, K.; Loccufier, M.; Verstockt, S.; Van de Walle, R.; Van Hoecke, S. Convolutional Neural Network Based Fault Detection for Rotating Machinery. *J. Sound Vib.* **2016**, *377*, 331–345. [CrossRef]
20. Lin, S.C.; Su, S.F.; Huang, Y. A Time-frequency Signal-based Convolutional Neural Network Algorithm for Fault Diagnosis of Gasoline Engine Fuel Control System. In Proceedings of the 2019 International Conference on System Science and Engineering, ICSSE 2019, Dong Hoi, Vietnam, 20–21 July 2019; pp. 81–87. [CrossRef]
21. Yoo, Y.; Jeong, S. Vibration analysis process based on spectrogram using gradient class activation map with selection process of CNN model and feature layer. *Displays* **2022**, *73*, 102233. [CrossRef]
22. Zheng, Y.; Qiu, Z. An efficient method for flutter stability analysis of aeroelastic systems considering uncertainties in aerodynamic and structural parameters. *Mech. Syst. Signal Process.* **2019**, *126*, 407–426. [CrossRef]
23. Jung, H.; Kim, J.; Lee, S. Rotor Fault Diagnosis Using CNN-Based Transfer Learning with Spectrogram Analysis. *Electronics* **2023**, *12*, 480. [CrossRef]
24. Rocano, E.E. Aplicación de Algoritmos de Aprendizaje Supervisado Para la Clasificación de Fallos Mecánicos en un Motor de Encendido Provocado. 2023. Available online: http://dspace.ups.edu.ec/handle/123456789/24708 (accessed on 5 March 2026).
25. Balki, M.K.; Çavuş, V.; Duran, İ.U.; Tuna, R.; Sayin, C. Experimental Study and Prediction of Performance and Emission in an SI Engine Using Alternative Fuel with Artificial Neural Network. *Int. J. Automot. Eng. Technol.* **2018**, *7*, 58–64. [CrossRef]
26. Cay, Y. Prediction of a gasoline engine performance with artificial neural network. *Fuel* **2013**, *111*, 324–331. [CrossRef]
27. Zeng, W.; Khalid, M.A.S.; Han, X.; Tjong, J. A Study on Extreme Learning Machine for Gasoline Engine Torque Prediction. *IEEE Access* **2020**, *8*, 104762–104774. [CrossRef]
28. León, R.S.; Maldonado, J.L.; Contreras, R.W. Predicción de emisiones de CO y HC en motores Otto mediante redes neuronales. *INGENIUS* **2020**, *2020*, 30–39. [CrossRef]

29. Medina, J.P.; León, R. Empleo de Algoritmos de Machine Learning para la Detección de Fallos en el Sistema de Encendido y Admisión de Aire en un Motor Otto. Bachelor's Thesis, Universidad Nacional de Loja, Loja, Ecuador, 2025. Available online: https://dspace.unl.edu.ec/items/1362a4a6-f45b-4856-87a5-112d89a1de50 (accessed on 8 July 2025).
30. León, R.; Maldonado, J. Identificación de Patrones de Fallas Mecánicas Mediante Redes Neuronales Artificiales Para el Diagnóstico de Motores de Encendido Provocado. 2018. Available online: http://dspace.ups.edu.ec/handle/123456789/16161 (accessed on 5 March 2026).